

## Structural analysis and optimization of large cooling tower subjected to wind loads based on the iteration of pressure

Gang Li\* and Wen-bin Cao

Department of Engineering Mechanics, State Key Laboratory of Structural Analysis of Industrial Equipment,  
Dalian University of Technology Dalian 116024, China

(Received May 4, 2011, Revised March 14, 2013, Accepted April 24, 2013)

**Abstract.** The wind load is always the dominant load of cooling tower due to its large size, complex geometry and thin-wall structure. At present, when computing the wind-induced response of the large-scale cooling tower, the wind pressure distribution is obtained based on code regulations, wind tunnel test or computational fluid dynamic (CFD) analysis, and then is imposed on the tower structure. However, such method fails to consider the change of the wind load with the deformation of cooling tower, which may result in error of the wind load. In this paper, the analysis of the large cooling tower based on the iterative method for wind pressure is studied, in which the advantages of CFD and finite element method (FEM) are combined in order to improve the accuracy. The comparative study of the results obtained from the code regulations and iterative method is conducted. The results show that with the increase of the mean wind speed, the difference between the methods becomes bigger. On the other hand, based on the design of experiment (DOE), an approximate model is built for the optimal design of the large-scale cooling tower by a two-level optimization strategy, which makes use of code-based design method and the proposed iterative method. The results of the numerical example demonstrate the feasibility and efficiency of the proposed method.

**Keywords:** cooling tower; wind load; structural analysis; optimization design

---

### 1. Introduction

The natural draught cooling tower is widely used in thermal power stations and other industrial fields. In general, the large-scale cooling tower is a thin-walled structure of reinforced concrete, supported with columns at the bottom. To improve the cooling efficiency and land utilization, the cooling towers are built higher and higher, with the highest cooling tower of 200m high in the world (Busch *et al.* 2002, Wu 1996). Such hyperbolic elastic thin-walled structure is sensitive to wind loads. During the past 50 years, some failures of the cooling towers have happened due to improper design, e.g., the cooling towers at Ferry Bridge in England in 1965, at Ardeer in Scotland in 1973, at Bouchain in Northern France in 1979 and at Fiddler's Ferry in England. The wind-induced response of cooling tower is the key factor to improve safety and to reduce tower crack (Chen *et al.* 2005). At present, the research on the large cooling towers is focused on the material properties of the shell structure of tower, such as multi-layered nonlinear concrete shell (Hyuk 2006, Waszczyszyn *et al.* 2000, Jurkiewicz *et al.* 1999), and the structural behavior under external environment (Viladkar *et*

---

\*Corresponding author, Professor, E-mail: [ligang@dlut.edu.cn](mailto:ligang@dlut.edu.cn)

al. 2006, Noorzaei *et al.* 2006), especially under wind loads.

In general, there are three ways to analyze the wind-induced response of the cooling tower. The first way is to obtain the wind pressure coefficient, the shape factors and the wind-induced vibration coefficient based on the experiments (Shi *et al.* 1979, Li *et al.* 2007). For example, the wind pressure coefficient of the tower can be approximated as a trigonometric series, which is unchanged along the height of the tower in the design specifications for cooling towers (GB 50009-2001 2002, GB/T 50102-2003 2003). The second way is to calculate the wind pressure and velocity distribution directly based on CFD (computational fluid dynamics) analysis with the appropriate turbulence model (Rafat 2010, Meroney 2006), by which the pressure distribution of the entire tower surfaces can be predicted. The third way is to perform spectral analysis with a variety of wind spectra of the tower. For the analysis of the cooling tower subjected to mean wind pressure, the first two ways have been applied. However, the work reported in the literature on the analysis of cooling towers subjected to wind load failed to consider the types of wind load due to the deformation of cooling tower. Because such a hyperbolic thin-walled structure is sensitive to wind load, the wind load is relative to the shape of structure. Furthermore, the effect of airflow inside the tower was also neglected in the current research.

Because the analysis of cooling tower is time-consuming, a surrogate based optimization strategy is employed with the approximate model, in which the design of experiments (DOE)(Montgomery 2008) is used to determine the relationship between structural response and design variables. Then, an approximate model with Radial Basis Function (RBF) can be obtained for the optimization of cooling tower, based on which the structure of cooling tower is optimized using genetic algorithm (GA)(Holland 1975)and non-linear programming by quadratic Lagrangian (NLPQL). The results of the numerical example demonstrate the feasibility and efficiency of the proposed method.

To deal with these problems, an iterative method has been developed in this paper, which uses steady CFD simulation to obtain the mean wind load, and FEM method to complete the structural analysis of cooling tower. An iterative procedure is proposed between CFD solver and FEM solver to update the wind load according to the deformation of cooling tower. The comparative study of the results obtained from the code regulations and iterative method is conducted. Based on the design of experiment (DOE), an approximate model is built for the optimal design of the large-scale cooling tower by a two-level optimization strategy, which makes use of code-based design method and the proposed iterative method. The results of the numerical example demonstrate the feasibility and efficiency of the proposed method.

## 2. Formulation of the fluid-structure interaction analysis of the cooling tower

Fig. 1 shows the coupling computational model of the cooling tower, in which both CFD simulation and structural analysis are performed. The  $k-\varepsilon$  turbulent model (Mohammadi *et al.* 1993) is often used for the CFD simulation of cooling tower (Shen *et al.* 2007), and the governing equations of fluid can be written as

$$\begin{cases} \frac{\partial U_i}{\partial x_i} = 0 \\ U_j \frac{\partial U_i}{\partial x_j} = -\frac{1}{\rho} \frac{\partial p}{\partial x_i} + \frac{\partial}{\partial x_j} \left( \nu \frac{\partial U_i}{\partial x_j} \right) + \frac{\partial}{\partial x_j} \left( -\overline{u_i u_j} \right) \end{cases} \quad (1)$$

where,  $i,j=1,2,3$ .  $U_i$ ,  $p$ ,  $\nu$ ,  $\overline{u_i u_j}$  are the mean velocity component, the pressure, the fluid dynamic viscosity and Reynold stress. For the  $k-\varepsilon$  model

$$\overline{u_i u_j} = \frac{2}{3} k \delta_{ij} - 2C_{\mu} k S_{ij} \tag{2}$$

where  $\delta_{ij}$  is Kronecker delta,  $C_{\mu}$  is the empirical constant,  $S_{ij}$  is the deviatoric stress. The control equations of turbulent kinetic energy  $k$  and turbulent dissipation rate  $\varepsilon$  can be expressed as

$$\begin{cases} U_j \frac{\partial k_i}{\partial x_i} = \frac{\partial}{\partial x_j} \left[ \left( \nu + C_k \frac{k^2}{\varepsilon} \right) \frac{\partial k}{\partial x_j} \right] - \overline{u_i u_j} \frac{\partial U_i}{\partial x_j} - \varepsilon \\ U_j \frac{\partial \varepsilon}{\partial x_j} = \frac{\partial}{\partial x_j} \left[ \left( \nu + C_{\varepsilon} \frac{k^2}{\varepsilon} \right) \frac{\partial \varepsilon}{\partial x_j} \right] - C_{\varepsilon 1} \frac{\varepsilon}{k} \overline{u_i u_j} \frac{\partial U_i}{\partial x_j} - C_{\varepsilon 2} \frac{\varepsilon^2}{k} \end{cases} \tag{3}$$

where  $C_{\mu}=0.09, C_k=0.09, C_{\varepsilon}=0.07, C_{\varepsilon 1}=1.44, C_{\varepsilon 2}=1.92$ .

The structural analysis of tower subjected to the mean wind load is static, with the equation as

$$\mathbf{K} \mathbf{u}_s = \mathbf{f} + \mathbf{f}^{ex} \tag{4}$$

where  $\mathbf{K}$  is the stiffness matrix;  $\mathbf{f}$  is the fluid load imposed on the structure;  $\mathbf{f}^{ex}$  is other external loads, such as gravity force. Using the FEM method, such as ANSYS software, Eq. (4) can be solved conveniently. For the fluid equations, FLUENT code and CFX code can be used.

In the paper, the CFD simulation is steady and the pressure of airflow on the surface of the cooling tower can be computed by steady CFD. Then, the boundary condition of airflow is updated according to the deformation of the structure under the wind load; therefore the CFD analysis will be executed again to compute the wind load. Fig. 2 shows the flowchart of the iterative method.

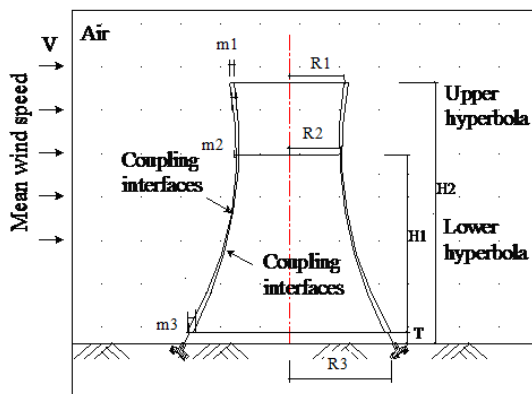


Fig. 1 Computational model of cooling tower

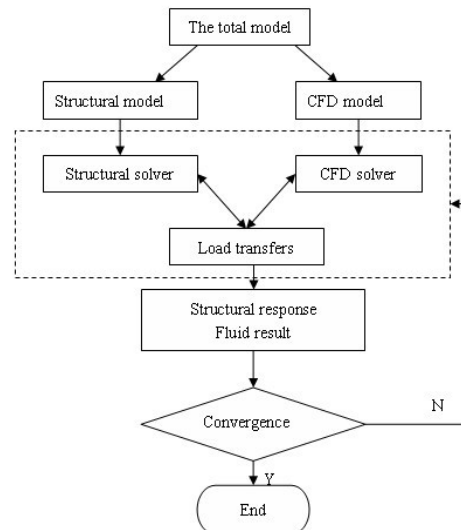


Fig. 2 the interaction flow

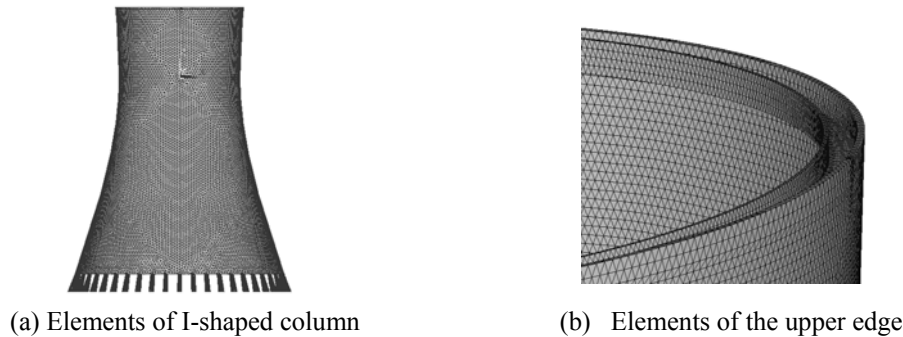


Fig. 3 Details of the local structure

Table 1 Geometry and material parameters

Parameter	Value	Meaning	Parameter	Value	Notation
$H1$ (m)	120.976	Throat height	$ca\_r$	2.000	R1-R2
$H2$ (m)	161.301	Total height	$Zn$	48	Number of columns
$R3$ (m)	62.039	Bottom radius	$Tan\phi$	0.348	Tangent of the angle between the bottom edge and the vertical axis
$R2$ (m)	34.120	Throat radius	$R3$ (m)	62.039	Bottom radius
$R1$ (m)	36.120	Top radius	$m3$ (m)	1.100	Thickness of the bottom
$T$ (m)	9.926	Column height	$m2$ (m)	0.250	Thickness of the neck
$RHSS$	1.300	$H2/(2 \times R3)$	$m1$ (m)	0.350	Thickness of top
$RSH$	0.750	$H1/H2$	$U_0$ (m/s)	26.000	Mean velocity
$RTSS$	0.080	$T/(2 \times R3)$	$E$ (GPa)	32.500	Elastic modulus
$RASS$	0.550	$H1/(2 \times R3)$	$\mu$	0.200	Poisson's ratio
$P$ (Kg/m <sup>3</sup> )	2500	Density of tower			

### 3. Model of the cooling tower and airflow

#### 3.1 FEM model of the tower structure

The relevant parameters of the cooling tower are shown in Table 1. The shell thickness of the cooling tower varies with the height. Usually, the generatrix equation of tower is not a standard hyperbolic equation but an offset hyperbolic equation or multi-segment offset hyperbolic equation, in order to meet the thermal and mechanical properties of cooling tower. As illustrated in Fig. 1, the meridional shape of a hyperbolic cooling tower consists of a lower and an upper hyperbola branches, connected at the throat. For the finite element model of cooling tower the second-order tetrahedral elements are used for the shell structure, as shown in Fig. 3.

#### 3.2 Model of the airflow

The CFD domain is a cylindrical domain, in which the radius is five times  $R3$  and the height is three times the height of cooling tower. The cooling tower is at the center of the computational domain, as shown in Fig. 4. The terrain roughness is type B according to the current Chinese code.

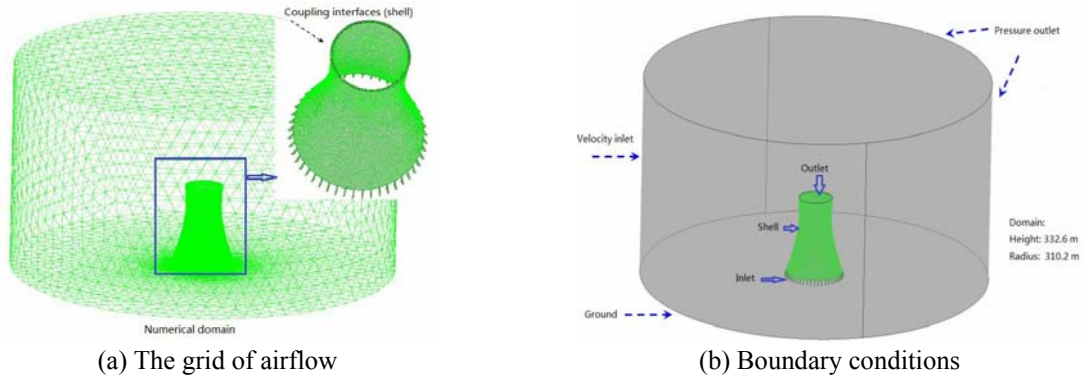


Fig. 4 The CFD model of the cooling tower

The inlet boundary conditions for fluid are calculated by the speed and turbulence intensity distribution model, which are defined in Eqs. (5) and (6) with the mean speed  $U_0$  of 26m/s. The outlet boundary condition is atmospheric pressure.  $k-\varepsilon$  model is used for CFD analysis of cooling tower, and the CFD model with 1,251,785 elements is used in the paper. The interfaces of the structure and fluid are that of the tower and air.

The CFD boundary conditions are composed of the wind speed distribution and turbulence intensity distribution. The wind speed distribution obeys exponential distribution (Architectural Institute of Japan 1996).

$$U_z = U_0 \left( Z/Z_0 \right)^\alpha \quad (5)$$

where  $Z_0$  and  $U_0$  are the reference height (10m) and the mean wind speed corresponding to the height,  $\alpha$  is the terrain roughness factor. For the type B of terrain roughness according to the current Chinese code,  $\alpha$  is 0.16. Turbulence intensity at the entrance is presented as

$$I_u = A \left( \frac{Z}{H} \right)^{-\alpha-0.05} \quad (6)$$

in which  $A$  is a constant,  $H$  is the atmospheric boundary layer height. As for  $I_u$ , it should be up to 16% at the height of 30m above the ground. The detail boundary conditions are shown in Fig. 4.

## 4. Structural analysis of cooling tower by the iterative method

### 4.1 Comparison of three analysis methods

In the paper, three analysis methods of wind load are studied and compared, the proposed iterative pressure method with fluid-structure interaction, the design code based method and the rigid body method (the conventional CFD method assuming the tower structure as a rigid body in CFD analysis) without fluid-structure interaction. The cooling tower is elastic for the structural analysis under the wind load obtained by the above three methods, respectively.

The design code based method (GB 50009-2001 2002, GB/T 50102-2003 2003) can be expressed as

$$\begin{cases} q(z, \theta) = \beta C_p(\theta) K(z) q_0 \\ C_p(\theta) = \sum_{n=0}^7 a_n \cos(n\theta) \end{cases} \quad (7)$$

where,  $q(z, \theta)$  is the pressure distribution on the outer surface of the tower shell;  $\beta$  is the wind fluttering factor;  $C_p(\theta)$  is the pressure distribution function;  $K(z)$  is the coefficient of wind pressure with height  $z$ ;  $q_0$  is the reference wind pressure,  $\theta$  is the horizontal angle measured from the windward meridian and  $a_n$  is the harmonic constant.

The result of the iterative method is compared with those by the code based method (Table 2), and with those by the rigid body method (Table 3). Fig.5 shows the iteration history of the responses of the cooling tower.

Table 2 Comparison of the iterative method and code-based method

Responses	Details	Iterative method	Code	Error (%)
Maximum displacement	Value /m	0.019	0.021	9.5
	Relative height	0.791	0.719	
	Windward angle /degree	0	0	
Maximum tension stress of shell	Value /MPa	3.100	3.370	8.0
	Relative height	0.344	0.591	
	Windward angle /degree	0	0	
Maximum compression stress of shell	Value /MPa	0.416	0.770	46.0
	Relative height	0.789	0.785	
	Windward angle /degree	9.053	0.00	

\*Error = absolute value of the (iterative method - Code)/Code

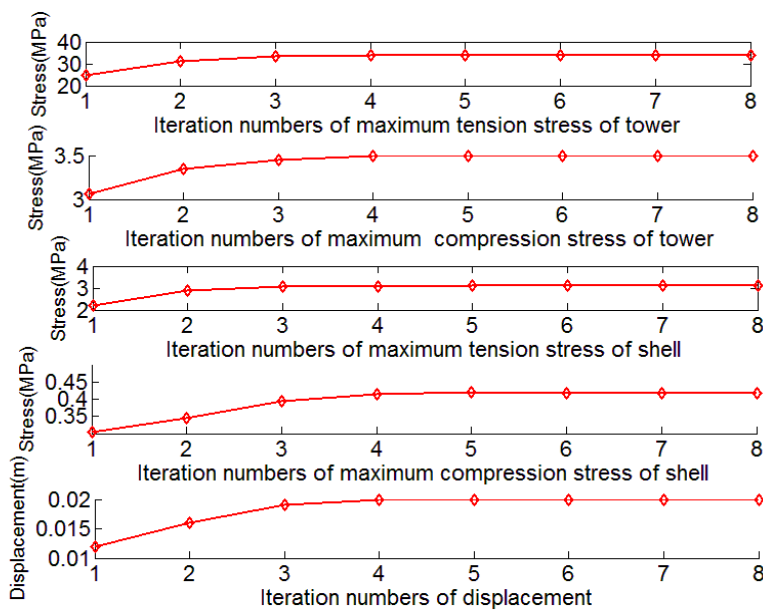


Fig. 5 The iteration history of responses by iterative method

Table 3 Comparison of the iterative method and the rigid method

	Details	Iterative method (with interaction)	Rigid model (without interaction)	Error (%)
Wind load	Total force(KN)	5700	5500	3.6
	Value (MPa)	3.1	2.87	8.0
Maximum tension stress of shell	Relative height	0.344	0.35	
	Windward angle /degree	0	0	
Maximum compression stress of shell	Value (MPa)	0.416	0.344	20.9
	Relative height	0.789	0.746	
	Windward angle /degree	9.053	10.1	
Maximum displacement	Value (m)	0.019	0.016	18.8
	Relative height	0.791	0.793	
	Windward angle /degree	0	0	

\*Error = absolute value of the (iterative method - Rigid model)/ Rigid model

Due to the particularity of the shape tower, a greater uplift force can be obtained, when the wind flows through the cooling tower. By calculation and analysis, the uplift force can be close to the weight of tower. As a result, the Maximum tensile stresses have much larger value than the maximum compressive stresses of the tower.

Although the displacements are very small to the height of the tower, they do cause some change of the shape of the tower structure, as shown in Figs.6-9. Since the wind load is very sensitive to the shape of tower, resulting in the different distribution of the wind pressure. The total wind force increases by 3.6%, when computing the wind load with fluid-structure interaction, as shown in Table 3.

The difference in wind load causes the increases of the structural responses. For example, the maximum tension and compression stress of shell are 3.1MPa and 0.416MPa for the iterative method (with fluid-structure interaction), 2.87MPa and 0.344MPa for the rigid method (without fluid-structure interaction), respectively. Thus, comparing the results of the two methods, the error is 8.0% for tension stress, 18.8% for displacement and 20.9% for compression stress. It should be pointed out that the absolute values of the structural responses (e.g., the displacement, compression stress) are quite small, and a slight change in the absolute values may cause a relatively big change in the error percentage. Furthermore, the error of the compression stress in the whole structure is within 7%, except for the region of the maximum stress.

Figs. 6-9 show the differences in results among the three methods. The displacement by the code based method is larger than those of the other two methods at 0-degree windward angle, while the displacement by the iterative method is the largest at 180-degree and 90-degree windward angle. The difference is gradually increasing from 90 degree to the leeward regions. Furthermore, the radial displacements of the structure are up to the maximum value nearby the neck of the tower for all the three methods.

Overall, according to Table 2 and Figs. 6-9, the code based method is conservative.

#### 4.2 Influence of the different wind speed on the response of cooling tower

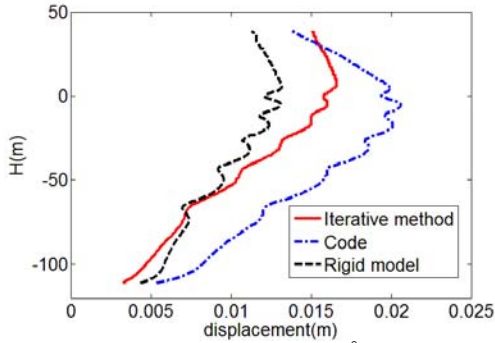


Fig. 6 Displacement vs height at 0° windward angle

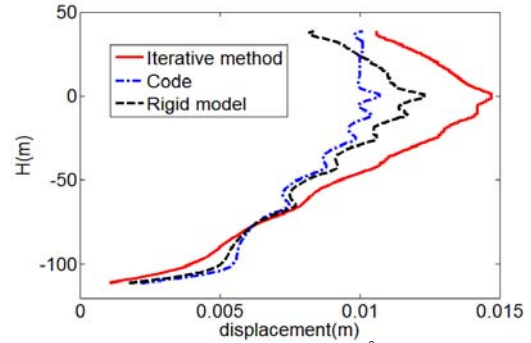


Fig. 7 Displacement vs height at 90° windward angle

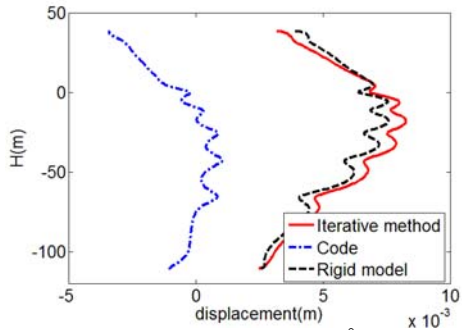


Fig. 8 Displacement vs height at 180° windward angle

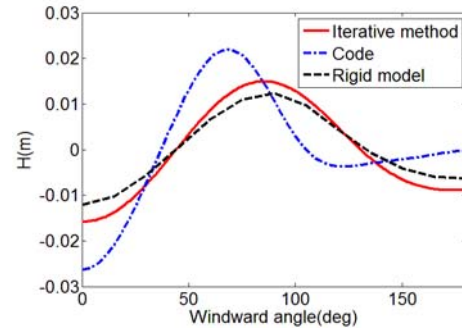


Fig. 9 Displacement of throat

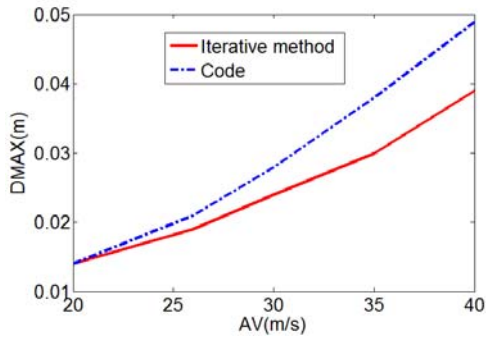


Fig. 10 Wind speed vs DMAX (Max displacement)

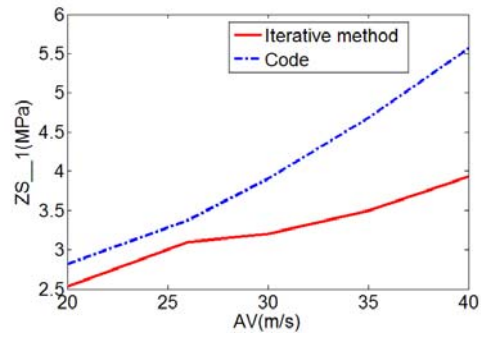


Fig. 11 Wind speed vs ZS\_1 (Maximum tension stress of shell)

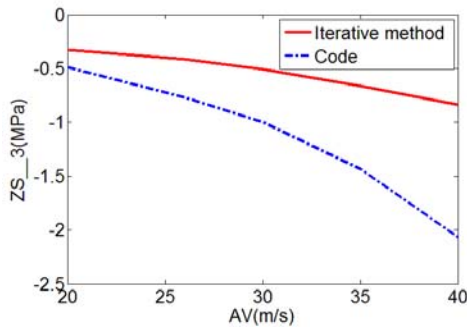


Fig. 12 Wind speed vs ZS\_3 (Maximum compression stress of shell)

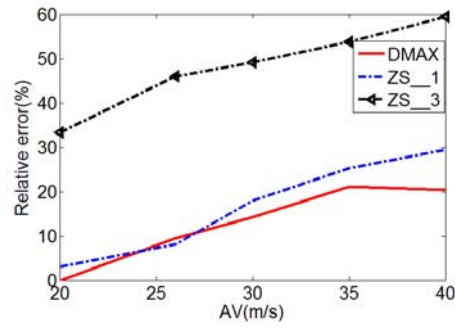


Fig. 13 Relative error

For different mean wind speed, the maximum response obtained by the proposed iterative method and code based method are studied and compared. Overall, the results of the code based method, which is relatively conservative, are larger than those of the iterative method, as shown in Figs. 10-12. Relative error becomes bigger with the increase of the mean wind speed, as shown in Fig. 13.

#### 4.3 Influence of inside airflow on the response of the cooling tower

Currently, there are few studies on the effects of the inside airflow of the cooling tower on the structure behaviour, especially when taking into account the effects of both inside and outside airflow of the tower. The above studies are focused on the natural draft dry cooling tower (NDDCT), which does not take into account the fill of inside of the tower. In this section, two kinds of computational model have been studied and compared for the effects of the inside airflow of the cooling tower on the structure behaviour: Model A fails to take into account the wind load of the inside airflow; Model B is the natural draft wet cooling tower (NDWCT), in which the fill has been computed. The resistance characteristics of fill materials are given as follows (Zhao 2006)

$$\frac{\Delta P}{\gamma_a} = A_p v^M \quad (8)$$

where  $\Delta P$  is the resistance of the fill,  $N/m^2$ ,  $\gamma_a$  is the specific gravity of the air,  $N/m^3$ ,  $v$  is the wind speed through the fill,  $m/s$ .  $A_p$  and  $M$  can be calculated by Zhao (2006)

$$A_p = 2.78 \times 10^{-2} q^2 + 0.877; \quad M_p = 3 \times 10^{-4} q^2 - 1.11 \times 10^{-2} q + 2 \quad (9)$$

where  $q$  is the water flow rate. A kind of dual-ramp material (Zhao 2006) is used at the height of 1.5m, with two cases of  $q=15m^3/(m^2 \cdot h)$  and  $q=8m^3/(m^2 \cdot h)$  considered. For the NDWCT, the influence of fill on the airflow will be taken into account with Darcy's law as follows

$$-\frac{\partial p}{\partial x_i} = \frac{\mu}{k_p} U_i + k_l \frac{\rho}{2} |U| U_i \quad (10)$$

where  $\mu$  is the dynamic viscosity,  $k_p$  is the permeability,  $k_l$  is the empirical loss coefficient. The CFD boundary condition of the NDWCT is the same to that of the NDDCT with mean wind speed 26m/s.

Table 4 Comparison of response of tower among various models

	NDWCT ( $q=8m^3/(m^2 \cdot h)$ )	NDWCT ( $q=15m^3/(m^2 \cdot h)$ )	NDDCT	Model A (without regard to the wind load of inside air)
ZS_1 (the maximum tension stress of the shell) (MPa)	3.080	3.082	3.100	3.110
ZS_3 (the maximum compression stress of the shell) (MPa)	-0.386	-0.388	-0.416	-0.396
DMAX (Max displacement) (m)	0.015	0.015	0.019	0.014
The relative altitude where ZS_1 takes place	0.340	0.340	0.344	0.344
The relative altitude ZS_3 takes place	0.810	0.810	0.789	0.791
The relative altitude where DMAX takes place	0.819	0.819	0.791	0.786

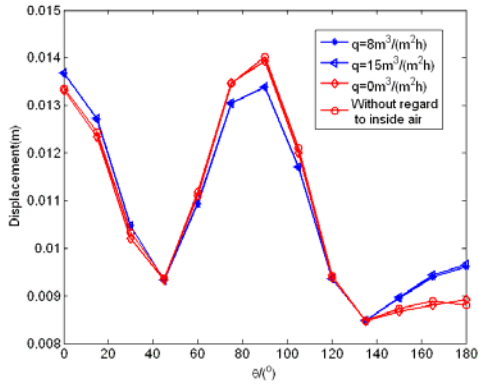


Fig. 14 The displacements of neck

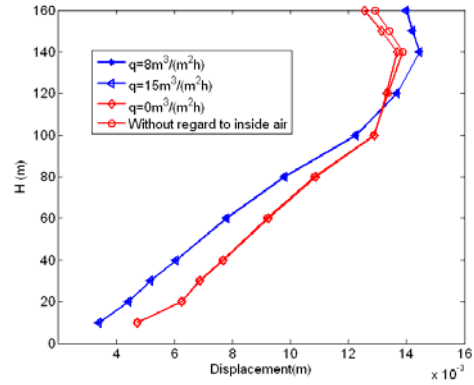


Fig. 15 Variation of displacements of tower along 0° meridian

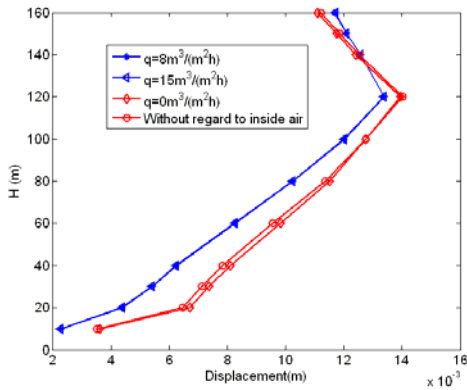


Fig. 16 Variation of displacements of tower along 90° meridian

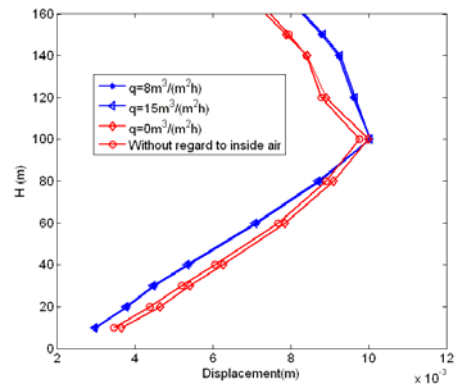


Fig. 17 Variation of displacements of tower along 180° meridian

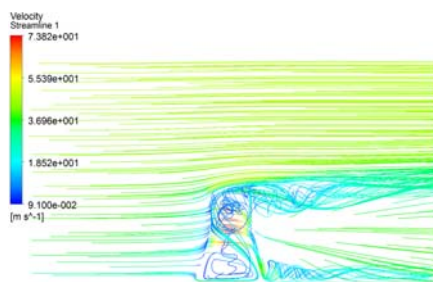


Fig. 18 Track in steamwise direction

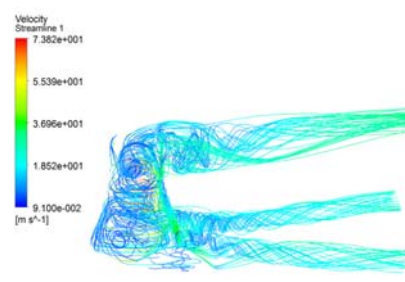


Fig. 19 Track from the surfaces of tower

According to Table 4 and Figs. 14-17, some differences among these models can be found: (1) For the NDWCT (model B), the water flow rate has little effect on the response of tower; (2) The results of Model A and the model NDDCT are very similar. Overall, the results of four models are approximate, so that the control wind load is the that of the outside surface of tower. Moreover, the peaks of displacement of tower take place nearby the neck for all models, which coincides with the Viladkar's research (2006).

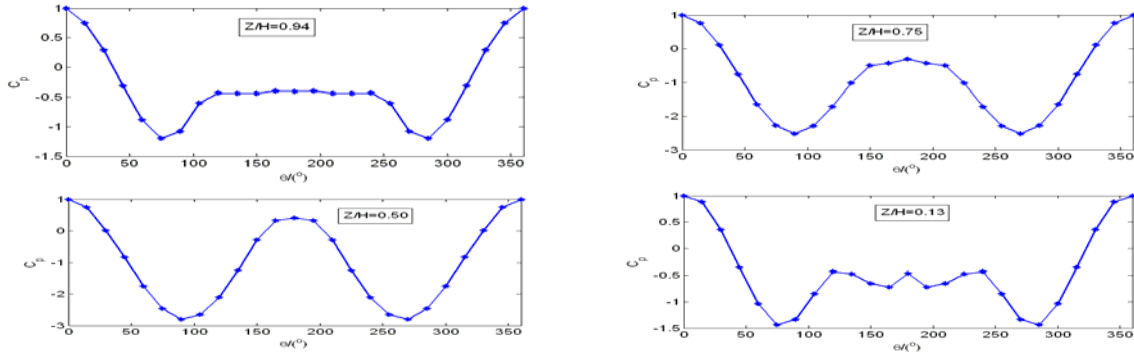


Fig. 20 Variation of surface wind pressure coefficient with azimuth at various height

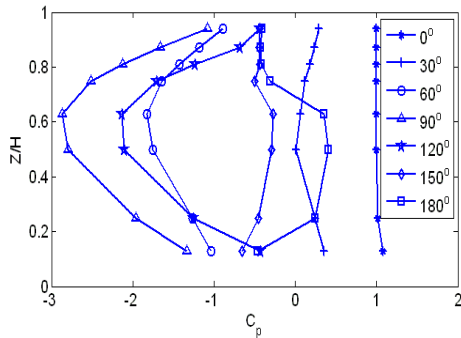


Fig. 21 Variation of surface  $C_p$  with height at various azimuth

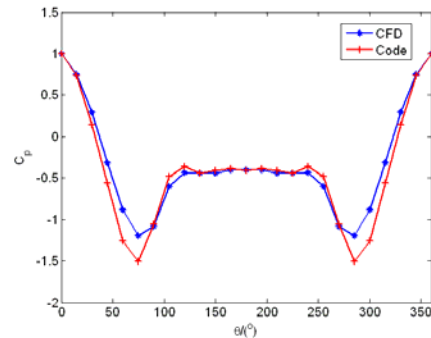


Fig. 22 Comparison between CFD and code data at 145m

#### 4.4 The analysis of airflow of the tower

Fig. 18 shows the airflow track in the streamwise direction, and the track from the surfaces of tower is shown in Fig. 19. The flow state is complex and turbulence takes place near the exit and interior of the tower, which may cause some influence on a group of towers. In general, the turbulence makes the wind pressure uniform, so the pressure coefficient  $C_p$  becomes uniform relatively at the lee near the exit and bottom of the outside surface of tower (from  $\theta=120^\circ$  to  $\theta=240^\circ$ ), as shown in Fig. 20 and Fig. 21, which can be obtained by

$$C_p(\theta, z) = \frac{p(\theta, z) - p_\infty(z)}{0.5\rho V_\infty^2(z)} \tag{11}$$

where  $p(\theta, z)$  is the pressure at the height  $z$  and the horizontal angle  $\theta$ ;  $p_\infty(z)$ ,  $V_\infty(z)$  and  $\rho$  are the static pressure, wind speed and density of the infinite air flow at the height  $z$ , respectively. According to Fig. 21, the maximum value of  $C_p$  takes place near the height of tower neck with  $z/H$  as 0.75.

Fig. 22 is the comparison of  $C_p$  by CFD and code (obtained by Eq. (7)) at the height of 145m, where turbulence is fully developed. There is a close correspondence between them, and there are two relative independent turbulent zones at the inside tower, which is consistent with the solution in Bao *et al.* (2009). The causes of the differences of the results mainly lie in that in the code based

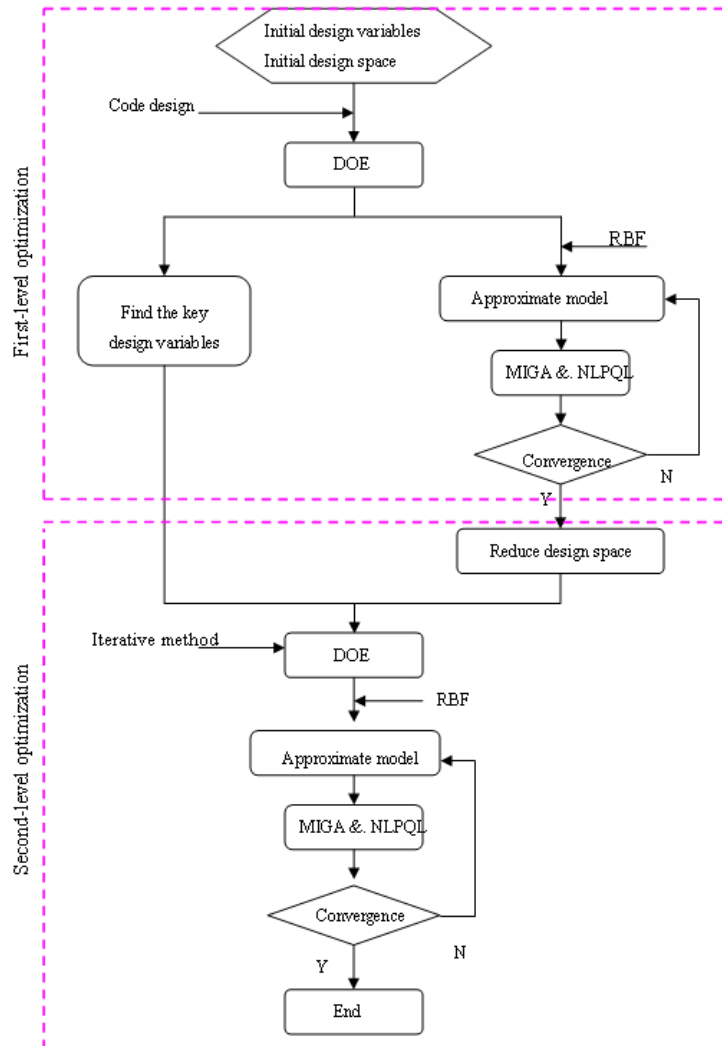


Fig. 23 The optimal flow chart

method, (1)  $C_p$  is assumed constant with height, (2) the fluid-solid interaction fails to be taken into account, and (3) the effect of columns on air flow fail to be computed. There are also some computational errors in the CFD simulation.

## 5. Structural optimization design of the cooling tower

Because of the special design and construction, the bottom ring girder and columns can have good mechanical properties for the safety of structure. So, for the structural optimization design in this paper, the maximum stresses of the shell are served as one of constraints, such as the maximum tension stress and compression stress of the shell.

Given the structural and fluid analysis system as a whole, the computational effort is much expensive due to the complex three-dimensional computational fluid dynamics. A two-level optimization strategy, which makes use of the standard design method (GB 50009-2001 2002, GB/T 50102-2003 2003) and the iterative method, is proposed to improve the efficiency of the optimization, as shown in Fig. 23. The Multi-Island Genetic Algorithm (MIGA) is used to optimize the approximations obtained by design of experiments (DOE) globally in order to obtain globally optimal solution. Then, non-linear programming by quadratic Lagrangian (NLPQL) method will be used to improve the optimal results of MIGA method. The optimal results are obtained under the platform of iSIGHT to call the analysis of code-based and iterative method.

In the first-level optimization, based on the analyses of DOE, the key variables can be identified and the initial design point can be obtained for the second-level optimization. In the second-level optimization, the design space can be reduced properly and rebuilt near the first-level optimal results. The constraints of first-level optimization and second-level optimization are shown in Table 6. Then through DOE analysis nearby design space of the results of the first-level optimization, the approximate model can be built by Radial Basis Function (RBF) technique based on the samples of previous DOE. The optimization model can be expressed as

$$\begin{aligned} \text{find } \mathbf{X} &= (x_1, x_2 \cdots x_n)^T & (12) \\ \text{min. } & f(\mathbf{X}) \\ \text{s.t. } & g_i(\mathbf{X}) \leq 0 \quad (i=1, \dots, M) \end{aligned}$$

where the vector  $\mathbf{X}$  is the structural parameters, such as  $RSH$ ,  $RHSS$  and so on.  $f(\mathbf{X})$  is the optimization objective. The volume of material ( $V$ ) is chosen as the optimization objective in this paper, and  $g_i(\mathbf{X})$  is the constraint,  $M$  is the number of the constraints.

### 5.1 The first-level optimization

DOE is applied to find the relationship between input and output parameters, then the key variables can be found with the initial optimal value for the first level optimization. The approximate model can be built by RBF technique based on the samples of DOE.

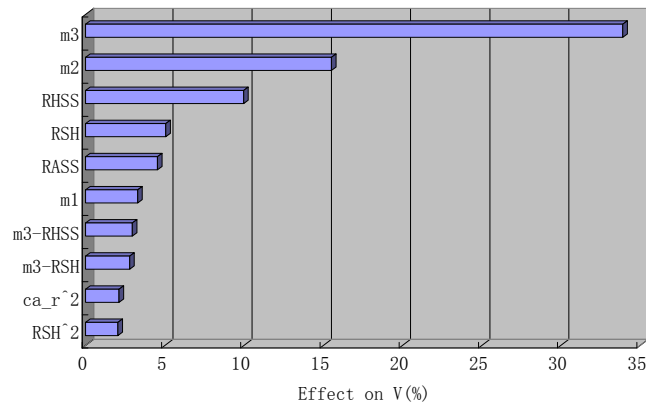
Because of the simplicity and efficiency of the code design, the code design has been used for the analysis of cooling tower. Then, based on the code design and approximate model, an optimal value can be obtained by the Multi-Island Genetic Algorithm and NLPQL method, the optimal results will be used as the original values of the second level, so that the better optimal results can be obtained.

#### 5.1.1 Analysis of DOE based on the code design

Through the above analysis, the maximum tension stress of the shell ( $ZS_1$ ) does not meet the constrain, the structure need to be designed and optimized to meet the design requirements. Based on code method, DOE analysis is executed by the technique of optimal Latin hypercube in the design space with 82 samples. As mentioned previously, the parameters of  $ca_r$ ,  $m1$ ,  $m2$ ,  $m3$ ,  $RASS$ ,  $RHSS$ ,  $RSH$ ,  $RTSS$  are selected as the design variables, according to the characteristics of the cooling tower. The parameters of  $RASS$ ,  $RHSS$ ,  $RSH$  and  $RTSS$  must meet the constraints (Liu 2000) of Table 6 in order to meet the thermodynamic performance of the cooling tower. Taking into account of the requirements (constraints) of the performance and the practical cases,  $g_i(\mathbf{X})$  is shown in Table 5. The Eq. (12) can be defined as

Table 5 Requirements (constraints) of the performance

Parameters	First-level optimization		Second-level optimization	
	lower	Upper	Lower	Upper
$ca\_r$ (Difference between neck radius and the top radius ) (m)	0.5	2.5	/	/
$m1$ (Thickness of top) (m)	0.2	0.5	0.2	0.3
$m2$ (Thickness of the neck) (m)	0.16	0.5	0.2	0.3
$m3$ (Thickness of the bottom) (m)	0.6	1.5	0.8	1.5
$RASS$ (Ratio of the throat height to the bottom diameter)	0.5	0.6	0.51	0.55
$RHSS$ (Ratio of the total height $H2$ to the bottom diameter)	1.2	1.4	1.15	1.32
$RSH$ (Ratio of the throat height $H1$ to the total height $H2$ )	0.7	0.8	0.77	0.8
$RTSS$ (Ratio of the inlet height to the bottom diameter )	0.08	0.09	/	/
$FR\_1$ (Fundamental frequency) (Hz)	1		1	
$KB$ (Elastic stability coefficient)	5		5	
$ZS\_1$ (Maximum tension stress of the shell) (MPa)		2.50		2.50
$ZS\_3$ (Maximum compression stress of the shell) (MPa)		27.50		27.50
$SITA$ (The slope of $\tan\phi$ )	3.0	3.5	3.0	3.5

Fig. 24 Pareto Plot for Response  $V$ 

$$\text{find } \mathbf{X}=(ca\_r,m1,m2,m3,RASS,RHSS,RSH,RTSS)^T \quad (13)$$

$$\text{min. } V(\mathbf{X})$$

$$\text{s.t. } g_i(\mathbf{X}) \leq 0 \quad (i=1,\dots,M)$$

According to 82 samples, DOE analysis is executed by iSIGHT software. As a result, the result of the Main Effects analysis and Pareto analysis can be obtained based on DOE. The contribution of  $ca\_r$ ,  $RTSS$  on the objective function  $V$  can be neglected, as shown in Fig. 24, Fig. 25 and Fig. 26, and the influence of  $m3$  has the greatest impact on the objective  $V$ . Therefore, for the objective  $V$ ,  $ca\_r$  and  $RTSS$  are not necessarily taken as the design variables, and the appropriate  $ca\_r$ ,  $RTSS$  can be selected to make the first frequency higher.

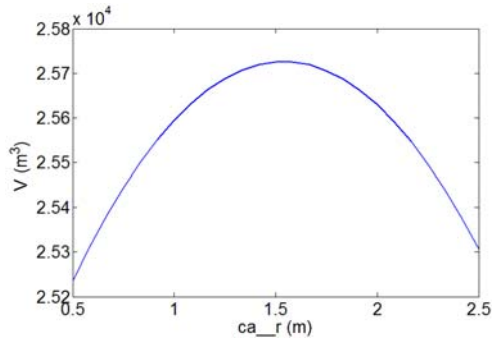
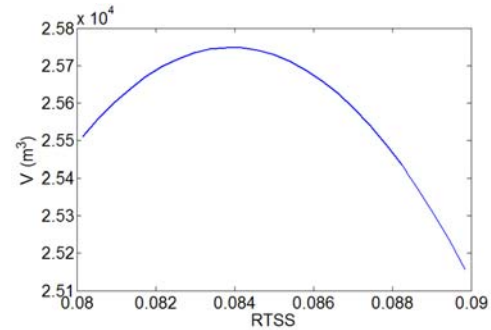
Fig. 25 Main Effects Plot for  $V$  about  $ca_r$ Fig. 26 Main Effects Plot for  $V$  about  $RTSS$ 

Table 6 Comparison of the precision of the first-level optimization based on the approximate model

Responses	First-level optimization (Result A)	FEM (Result B)	Error(%) $ B - A /A$
$FR_1$ (Fundamental frequency) (Hz)	1.1063	1.0893	1.54
$KB$ (Elastic stability coefficient)	5.6300	5.5525	1.38
$ZS_1$ (Maximum tension stress of the shell) (MPa)	2.2529	2.4841	10.3
$ZS_3$ (Maximum compression stress of the shell) (MPa)	0.5775	0.6944	20.22
$SITA$ (The slope of $\tan\varphi$ )	0.341	0.3419	0.226
$V$ (Volume of material) ( $m^3$ )	27865	27850.5	0.05

Table 7 Result of the first-level optimization based on approximate model

Parameters	Initial value	Result of first-level optimization
$ca_r$ (Difference between neck radius and the top radius) (m)	2.000	1.1331
$m1$ (Thickness of top) (m)	0.350	0.2371
$m2$ (Thickness of the neck) (m)	0.250	0.2116
$m3$ (Thickness of the bottom) (m)	1.100	1.3546
$RASS$ (Ratio of the throat height to the bottom diameter)	0.550	0.5340
$RHSS$ (Ratio of the total height $H2$ to the bottom diameter)	1.300	1.2770
$RSH$ (Ratio of the throat height $H1$ to the total height $H2$ )	0.750	0.7970
$RTSS$ (Ratio of the inlet height to the bottom diameter)	0.080	0.0862

### 5.1.2 Optimization design with the approximate model

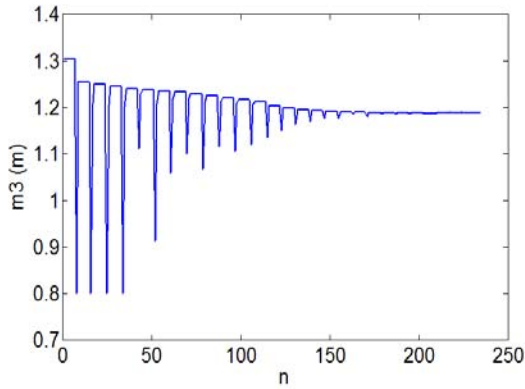
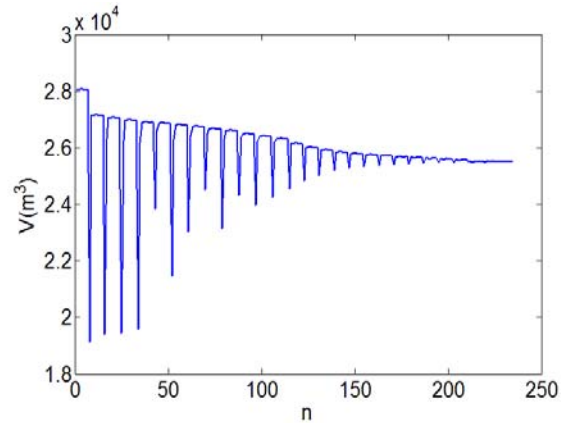
According to the results of the above DOE analysis, an approximate model can be constructed using RBF method. For the optimization, the MIGA has been applied firstly based on approximate model, then NLPQL method has been used to improved the accuracy of the optimal result of MIGA. According to Table 6, the optimal results of the approximate model are very close to the results of FEM. Table 7 shows the result of the first-level optimization.

### 5.2 The second-level optimization

Based on the first-level optimal result, the iterative method is used to obtain more accurate

Table 8 Result of multi-island genetic algorithm

Parameter	<i>RSH</i>	<i>RASS</i>	<i>RHSS</i>	<i>m1</i>	<i>m2</i>	<i>m3</i>
Value	0.77799	0.5171	1.31693	0.23067	0.281	1.30449

Fig. 27 History of  $m_3$ Fig. 28 History of  $V$ 

optimal result combined with the approximation. As mentioned previously, the parameters of  $ca_r$  and  $RTSS$  can be confirmed by the first optimization based on the code method. So the values of  $ca_r$  and  $RTSS$  are fixed to 1.1331 and 0.0862, respectively. In addition, the design space can be reduced to improve to the efficiency and accuracy. The constraint  $g_i(\mathbf{X})$  is shown in Table 6. The optimal flow chart is shown in Fig. 23. According to Eq. (13), the new optimization model can be given by

$$\text{find } \mathbf{X}=(m_1,m_2,m_3,RASS,RHSS,RSH)^T \quad (14)$$

$$\text{min. } V(\mathbf{X})$$

$$\text{s.t. } g_i(\mathbf{X}) \leq 0 \quad (i=1,\dots,M)$$

The same DOE method is used for sampling in the design space by optimal Latin hypercube technique. 36 sample points obtained by DOE are used to construct the approximate model by RBF. Because the problem is a highly nonlinear multi-peak problem, the error of 3-order response surface model is up to 40% according to analysis; however, the error of the RBF model is less than 30%. So the RBF model is chosen in this paper.

For the optimization, the MIGA has been applied firstly with the results shown in Table 8, which is used as the initial point for the next optimization by NLPQL method in order to improve the accuracy of the optimal result. The final optimal result is compared with the result of iterative method to check the rationality and accuracy of optimal result. The iterative history of fitness (objective) using NLPQL based on the result of MIGA is shown in Fig. 27 and Fig. 28.

Table 9 Comparison of the precision of the second-level optimization based on the approximate model

Responses	Second-level optimization (Result A)	FEM (Result B)	Error(%) $ B-A /A$
<i>FR_1</i> (Fundamental frequency) (Hz)	1.0432	1.2150	14.1
<i>ZS_1</i> (Maximum tension stress of the shell) (MPa)	2.300	2.500	8
<i>ZS_3</i> (Maximum compression stress of the shell) (MPa)	0.2500	0.3600	30.6
<i>SITA</i> (The slope of $\tan\phi$ )	0.3500	0.3457	1.2
<i>KB</i> (Elastic stability coefficient)	7.5500	10.056	24.9
<i>V</i> (Volume of material ) (m <sup>3</sup> )	25508	26151	2.5

Table 10 The optimal result and initial design

	Initial design	First-level optimal result	Second-level optimal result
<i>ca_r</i> (Difference between neck radius and the top radius) (m)	2.000	1.133	1.133
<i>m1</i> (Thickness of top) (m)	0.350	0.237	0.200
<i>m2</i> (Thickness of the neck) (m)	0.250	0.212	0.234
<i>m3</i> (Thickness of the bottom) (m)	1.100	1.355	1.189
<i>RASS</i> (Ratio of the throat height to the bottom diameter)	0.550	0.534	0.518
<i>RHSS</i> (Ratio of the total height <i>H2</i> to the bottom diameter)	1.300	1.277	1.320
<i>RSH</i> (Ratio of the throat height <i>H1</i> to the total height <i>H2</i> )	0.750	0.797	0.782
<i>RTSS</i> (Ratio of the inlet height to the bottom diameter )	0.080	0.086	0.086
<i>FR_1</i> (Fundamental frequency) (Hz)	1.238	1.089	1.215
<i>KB</i> (Elastic stability coefficient)	10.250	5.550	10.056
<i>ZS_1</i> (Maximum tension stress of the shell) (MPa)	3.100	2.500	2.500
<i>ZS_3</i> (Maximum compression stress of the shell) (MPa)	0.416	0.690	0.360
<i>SITA</i> (The slope of $\tan\phi$ )	0.348	0.342	0.346
<i>V</i> (Volume of material) (m <sup>3</sup> )	24577	27851	26151

From Table 9 and Table 10, the errors in the optimal results of the RBF approximate model are acceptable. The parameter *V* (Volume of material) of the second-level optimal result is 1600m<sup>3</sup> (6.1%) less than that of the first-level optimal result, meeting all the design constraints. Moreover, when the wind speed becomes stronger, the relative error becomes bigger, because the code method, which has been used for the first-level optimization, is relatively conservative. Thus, for the strong wind load, the second-level optimization has a better result based on the first-level optimization. On the other hand, the two-level optimization strategy is also fit for other engineering optimization problems.

## 6. Conclusions

In this paper, the structural analysis of the cooling tower has been completed firstly by the iterative pressure method, which combines CFD simulation and FEM in order to improve the accuracy of analysis. Then, based on RBF model, a two-level optimization strategy with better efficiency and higher accuracy has been proposed for the time-consuming analyses of cooling tower,

which combines code method and the iterative method.

(1) The code based method is conservative, and the relative error between iterative method and code based method becomes bigger with the increase of the mean wind speed, e.g., more than 30% for the mean wind speed of 35m/s. The main reason for the difference is that pressure coefficient  $C_p$  is constant along the height, according to the code method. On the other hand, for the conventional method of CFD with the model of rigid structure, the error is up to 25% according to the model stated in this paper.

(2) According to the iterative method, the pressure coefficient  $C_p$  becomes uniform relatively at lee near the exit and bottom of the outside surface of tower because of turbulence, which is different from Chinese code.

(3) There is less influence of the air inside the tower and the water distribution system on the structural response, so the wind load of the outside surface of tower is dominated.

(4) Corresponding to the results of DOE, the parameters of  $ca_r$  (the difference between neck radius  $R_2$  and the top radius  $R_1$ ) and  $RTSS$  (the ratio of the inlet height to the bottom diameter of the tower) have a minimum impact on the volume and the fundamental frequency of the tower, while  $m_3$  (thickness of the bottom) has a maximum impact.

(5) By the two-level optimization strategy, the structural design, which meets all the design constraints, can be obtained with good efficiency and accuracy.

## Acknowledgments

The support of the National Key Technology R&D Program (No.2006BAB03A07-02) is much appreciated.

## References

- Architectural Institute of Japan (1996), "Recommendations for loads on building", *Architectural Institute of Japan*, Tokyo.
- Bao, K.Y., Shen, G.H. and Sun, B.N. (2009), "Numerical simulation of mean wind load on large hyperbolic cooling tower", *Acta Aerodynamica Sinica*, **27**(6), 650-655.
- Bruno, J., Destrebecq, J.F. and Alain, V. (1999), "Incremental analysis of time-dependent effects in composite Structures", *Computers and Structures*, **73**, 425-435.
- Busch, D., Harte, R., Krätzig, W.B. and Montag, U. (2002), "New natural draft cooling tower of 200m of height", *Eng. Struct.*, **24**, 1509-1521.
- Chen, W.F. and Eric, M.L. (2005), *Handbook of structural engineering*, CRC Press, Boca Raton, New York.
- GB 50009-2001 (2002), *Load code for the design of building structures*, China Architecture & Building Press, China.
- GB/T 50102-2003 (2003), *Code for design of cooling for industrial recirculating water*, China Planning Press, China.
- Holland, J.H. (1975), *Adaptation in natural and artificial systems: An introductory analysis with applications to biology, control, and artificial intelligence*, University of Michigan Press, Michigan
- Hyuk, C.N. (2006), "Nonlinear behavior and ultimate load bearing capacity of reinforced concrete natural draught cooling tower shell", *Eng. Struct.*, **28**, 399-410.
- Li, J.Y., Ren, C.L. and Huang, Z.L. (2007), "Experiment study and finite element analysis of a natural draft cooling tower", *Chinese Quarterly of Mechanics*, **3**(28), 443-447.
- Liu, M.H. (2000), "Optimized calculation and model selection of double curved cooling towers", *Electric*

- Power Construction*, **10**, 35-41.
- Meroney, R.N. (2006), "CFD prediction of cooling tower drift", *Journal of Wind Engineering and Industrial Aerodynamics*, **94**, 463-490.
- Mohammadi, B. and Pironneau, O. (1993), *Analysis of the K-epsilon turbulence model*, Wiley, Chichester and New York and Paris.
- Montgomery, D.C. (2008), *Design and Analysis of Experiments, 7rded*, John Wiley and Sons, New York.
- Noorzai, J., Naghshineh, A., Abdul Kadir, M.R., Thanoon, W.A. and Jaafar, M.S. (2006), "Nonlinear interative analysis of cooling tower–foundation–soil interaction under unsymmetrical wind load", *Thin-Walled Structures*, **44**, 997-1005.
- Rafat, A.W. and Masud, B. (2010), "Cross winds effect on the performance of natural draft wet cooling towers", *International Journal of Thermal Sciences*, **49**, 218-224.
- Shen, G.H., Liu, R.F. and Sun, B.N. (2007), "Numerical simulation of wind load on cooling towers under double-tower condition", *Journal of Zhejiang University (Engineering Science)*, **41**(6), 1017-1022.
- Shi, Y.J. and Wang, D.Z. (1979), "Test method of cooling tower", *Thermal Power Generation*, **9**, 1-31.
- Viladkar, M.N., Karisiddappa, P.B. and Godbole, P.N. (2006), "Static soil–structure interaction response of hyperbolic cooling towers to symmetrical wind loads", *Eng. Struct.*, **28**, 1236-1251.
- Waszczyszyn, Z., Pabisek, E., Pamin, J. and Radwan´ska, M. (2000), "Nonlinear analysis of a RC cooling tower with geometrical imperfections and a technological cut-out", *Eng. Struct.*, **22**, 480-489.
- Wu, J.K. (1996), "Retrospect and prospect about structural analysis of large cooling tower", *Mechanics in Engineering*, **18**(6), 1-5.
- Zhao, S.A. (2006), *Salt water cooling tower*, China WaterPower Press, Bei Jing.